Crystallographic and NMR Investigation of Cobalt-Substituted Amicyanin[†,‡]

Christopher J. Carrell,[§] Xiaotang Wang,[||] Limei Jones,[⊥] William L. Jarrett,[#] Victor L. Davidson,[⊥] and F. Scott Mathews*[,§]

Department of Biochemistry and Molecular Biophysics, Washington University School of Medicine, St. Louis, Missouri 63110, Department of Chemistry, Jackson State University, Jackson, Mississippi 39217, Department of Biochemistry, University of Mississippi Medical Center, Jackson, Mississippi 39216, and Department of Polymer Science, School of Polymers and High-Performance Materials, University of Southern Mississippi, Hattiesburg, Mississippi 39406

Received February 18, 2004; Revised Manuscript Received May 7, 2004

ABSTRACT: Cobalt(II) amicyanin was prepared by replacing the copper of the type I copper protein amicyanin from *Paracoccus denitrificans* with cobalt. The structure of the protein and the metal center have been characterized by X-ray crystallography and paramagnetic NMR spectroscopy. The crystal structure indicates that Met98, which provides an axial sulfur ligand in native amicyanin, is no longer bound to the metal in cobalt(II) amicyanin and that a water molecule is recruited from solvent to form the fourth metal ligand. This results in a tetrahedral coordination geometry for the cobalt ion. NMR studies in solution also indicate that the side chain of the methionine residue interacts less strongly with the metal in *P. denitrificans* amicyanin than in *Paracoccus versutus* amicyanin. The cobalt(II) amicyanin crystal structure is different from that of cobalt-substituted azurin in which the carbonyl of a glycine residue provides this equivalent ligand. In cobalt(II) amicyanin that residue is a proline, for which the oxygen is structurally inaccessible, so that the water occupies the position held by the glycine carbonyl in cobalt(II) azurin. Such a metal coordination involving water has not previously been reported for a native or metal-substituted type I copper protein.

Amicyanin is a small type I blue copper protein that serves as an electron carrier between methylamine dehydrogenase (MADH)[1] and one or more soluble cytochromes in the periplasmic space of certain methylotrophic and facultative autotrophic bacteria, including *Paracoccus denitrificans* and *Paracoccus versutus* (formerly *Thiobacillus versutus*) (*1*, *2*). Expression of both MADH and amicyanin is induced when these organisms are grown on methylamine as the sole source of carbon and energy, and the genes which encode them are contained within the same methylamine utilization (*Mau*) operon (*3*). The structures of amicyanin from these two organisms have been determined by X-ray diffraction at 1.3 and 2.15 Å resolution, respectively (*4*, *5*). The protein has a molecular mass of about 12.5 kDa and folds as a β-sandwich, with nine β-strands forming two mixed β-sheets. The copper is located at one end of the β-sandwich and is coordinated by four protein side chain ligands, a cysteine, two histidines, and one methionine. The coordination geometry is a distorted tetrahedron with the copper lying close to the plane formed by the three equatorial ligands, one cysteine and two histidines, and the axial methionine ligand positioned somewhat further away.

Amicyanin is most closely related in structure to two other cupredoxins, plastocyanin and pseudoazurin (*6*, *7*), and shares with them a similar protein fold and copper coordination geometry. A central core of eight β-strands that form a "β-sandwich" is common to all three proteins and generally congruent (except for a few insertions) with amicyanin extending about 20 residues in the N-terminal direction and pseudoazurin extending about 30 residues in the C-terminal direction. Another well-studied cupredoxin, azurin (*8*, *9*), is less closely related to amicyanin and exhibits somewhat different coordination of the copper. In addition to the three equatorial cysteine and histidine ligands and the axial methionine ligand, it has a fifth ligand occupying a second axial position to form a trigonal bipyramid. The fifth ligand is the carbonyl oxygen atom of a glycine residue that is adjacent to one of the histidine ligands.

As cupredoxins generally serve in the capacity of electron carriers, the electronic structures of the copper redox centers of these proteins are of interest. NMR is a potentially useful technique to probe the electronic structure of protein active sites when a paramagnetic center is present (*10*). These centers can give rise to large chemical shifts of protons close to them, and the identities of the protons which give rise to these specific signals may be assigned on the basis of the protein structure. Unfortunately, the divalent copper center in most type I cupredoxins suffers a slow electronic relaxation rate that gives rise to excessive line broadening that degrades the NMR signals from nearby protons (*11*). One approach to overcome this problem has been to

[†] This work was supported by NSF Grant MCB-0091084 (F.S.M.), NIH Grant G12RR13459 (X.W.), and NIH Grant GM41574 (V.L.D.).

[‡] Crystallographic coordinates have been deposited in the Protein Data Bank under the file name 1TK5.

* Corresponding author. E-mail: mathews@biochem.wustl.edu. Phone: (314) 362-1080. Fax: (314) 362-7183.

[§] Washington University School of Medicine.

[||] Jackson State University.

[⊥] University of Mississippi Medical Center.

[#] University of Southern Mississippi.

[1] Abbreviations: MADH, methylamine dehydrogenase; RMSD, root mean square deviation.

10.1021/bi049635r CCC: $27.50
Published on Web 06/29/2004

substitute the copper of cupredoxins with divalent cobalt or nickel, which undergoes fast relaxation and gives rise to much sharper signals leading to more accurate assignments (*12*).

A number of spectroscopic and NMR studies of both cobalt- and nickel-substituted azurin and mutants of azurin have been described (*13*, *14*). When correlated with complementary crystal structure investigations, these studies indicate that the geometries of the cobalt and nickel centers shift so that the bond from the metal to the methionine sulfur weakens while the bond to the carbonyl oxygen strengthens. Recently, an NMR study of cobalt- and nickel-substituted amicyanin from *P. versutus* was reported (*15*). This study indicated that the coordination geometry of the substituted metals was very similar to that with copper but that the metal to methionine interaction was stronger than was observed in the analogous cobalt complex with azurin (*13*). In this paper we report the crystal structure and NMR investigation of cobalt-substituted amicyanin from *P. denitrificans.* The crystal structure indicates that the methionine is no longer bound to the metal in cobalt(II) amicyanin and that a water molecule is recruited from solvent to form the fourth ligand, resulting in a considerably more regular tetrahedral coordination geometry for the cobalt ion. Contrary to the results observed in *P. versutus* amicyanin, NMR studies of the cobalt(II) complex of *P. denitrificans* amicyanin indicate a weaker interaction between the methionine residue and the metal, as compared to that in the native protein. A metal coordination such as this involving water has not previously been reported for a native or metal-substituted type I copper protein.

MATERIALS AND METHODS

Preparation of Cobalt Amicyanin. Recombinant amicyanin was expressed in *Escherichia coli* and purified as described previously (*16*). To remove copper, amicyanin was first reduced with excess sodium dithionite and then dialyzed at 4 °C for 20 h against a solution of 0.1 M Tris-HCl, pH 8.0, containing 0.1 M KCN. The resulting apoamicyanin was then further dialyzed at 4 °C for 5 h against 10 mM Tris-HCl metal-free buffer, pH 7.5. The buffer was made metal-free by passage over a Chelex resin. Next a 20-fold molar excess of $CoCl_2$ was added to the apoamicyanin at room temperature and incubated on a 60 rpm shaker for 4 h. The reaction mixture was pink at first and then gradually changed to a green color. The cobalt(II) amicyanin was then subjected to gel filtration chromatography over ACA202 to remove any excess $CoCl_2$. Concentrations of cobalt(II) amicyanin were estimated from the known concentration of amicyanin prior to reconstitution and the known extinction coefficient at 280 nm for native amicyanin. Previously described procedures were used to purify MADH (*17*) and cytochrome *c*-551i (*18*) from *P. denitrificans*.

Kinetic Analyses. Steady-state kinetic experiments with MADH using amicyanin as the electron acceptor and with MADH and amicyanin using cytochrome *c*-551i as the electron acceptor were performed as described previously (*19*). The assay mixtures contained 16 nM MADH, varied amounts of amicyanin or cobalt(II) amicyanin, and 21 μM cytochrome *c*-551i, when present, in 10 mM potassium phosphate, pH 7.5. The reactions were initiated by the addition of 0.1 mM methylamine.

X-ray Crystallography. Cobalt(II) amicyanin was crystallized by a microbatch method using a nine-well Pyrex culture plate, as described previously (*20*), where 0.025 mL of cobalt(II) amicyanin (10 mg/mL) was mixed with an equal volume of a 9 to 1 mixture of monobasic sodium (4.0 M) and dibasic potassium (4.0 M) phosphate solution. Each well of the plate was then covered by 10 drops of mineral oil, and the plate was placed in a constant temperature chamber (20 °C). Microseeds of apoamicyanin obtained previously were added to the wells; faint green crystals formed within an hour and grew to a usable size within 1 week.

For data collection, crystals were transferred to paraffin oil to remove water from the crystal surface by blotting with a strand of filter paper. A blotted crystal was then frozen in a cryostream at 110 K using paratone oil (Hampton Research, Laguna Hills, CA) as a cryoprotectant. X-ray diffraction data were collected on an ADSC Quantum-4 CCD at the BIOCARS Beamline 14-BM-C at the Advanced Photon Source, Argonne National Laboratories, Argonne, IL. The HKL package (*21*) was used for data processing and scaling. X-ray diffraction data statistics are summarized in Table 1.

The structure of cobalt(II) amicyanin was solved by molecular replacement using the polypeptide chain from the 1.3 Å resolution structure of copper(II) amicyanin (PDB code 1AAC). All water molecules and the copper atom were removed from the probe model. The cross-rotation and translation functions were performed by the program MOLREP from the CCP4 suite (*22*), using all data to 3.5 Å resolution. Rigid-body refinement using data to 3.0 Å resolution was then carried out on the four independent molecules of cobalt(II) amicyanin in the asymmetric unit identified in MOLREP, using the program CNS (*23*). Atomic refinement using all data to 1.4 Å resolution was then performed using REFMAC (*24*) with cross-validation. Noncrystallographic symmetry restraints were not applied; water molecules were added during refinement to a total of 617 using ARP-wARP in CCP4 (*22*), and five phosphate ions were identified; model building was performed using XTALVIEW (*25*). The final value for R_{work}[2] was 0.182 and for R_{free}[2] was 0.211; a final cycle of refinement with all of the data included yielded R_{total}[2] = 0.184. The complete refinement statistics can be found in Table 1.

NMR Spectroscopy. Protein samples for NMR experiments were prepared in either D_2O buffer or 90% H_2O/10% D_2O buffer solutions by at least five isotope exchanges of the protein solution in H_2O with D_2O buffered at pH 7.4. The isotope exchanges were carried out in either Centricon or Centriprep tubes (both from Amicon, Inc.) at 4 °C. All NMR samples contained approximately 1.5 mM cobalt(II) amicyanin.

Proton NMR spectra of cobalt(II) amicyanin were recorded at 20 °C on a Varian Unity-Inova 500 FT NMR spectrometer operating at a proton frequency of 499.77 MHz. The residual solvent signal was suppressed with either the super WEFT method (*26*) or presaturation during relaxation delay. Chemical shift values were referenced to the residual HDO signal that was calculated according to the relationship of $\delta_T = \delta_{25} - 0.012(T - 25)$, where δ_T is the chemical shift of HDO at temperature T in degrees Celsius and δ_{25} is the chemical shift of HDO at 25 °C (*27*).

[2] See footnote *c* of Table 1 for a definition of R_{work}, R_{free}, and R_{total}.

Table 1: Data Collection and Refinement Statistics

Data Collection Statistics	
unit cell parameters	
a (Å)	57.70
b (Å)	56.40
c (Å)	58.71
β (deg)	99.67
space group	$P2_1$
max *d* spacing (outer shell) (Å)	1.40 (1.48−1.40)
mosaicity (deg)	0.45
no. of observations total	169057
no. of observations unique	71331
completeness (%)	97.8 (91.2)
multiplicity	2.4 (1.7)
R_{merge}[a]	0.052 (0.273)
average $I/\sigma(I)$[b]	15.3 (2.2)
Refinement Statistics	
no. of reflections in test set[c]	67713
no. of reflections in working set[c]	3619
R_{work}[d]	0.182
R_{free}[d]	0.210
R_{total}[d]	0.184
no. of protein atoms including Co	3244
no. of atoms in phosphate ions	25
no. of water molecules	617
RMSD bond length (Å)	0.018
RMSD bond angles (deg)	1.7
mean protein *B* factor (Å^2)	11.9
mean water *B* factor (Å^2)	25.2
mean cobalt *B* factor (Å^2)	14.1
mean phosphate *B* factor (Å^2)	28.2
RMS Δ*B* (m/m, Å^2)[e]	0.92
RMS Δ*B* (m/s, Å^2)[e]	0.96
RMS Δ*B* (s/s, Å^2)[e]	2.61
Estimated Standard Uncertainties (Å)	
Luzzati[f]	0.160
DPI[g]	0.087

[a] $I/\sigma(I)$ is the average signal-to-noise ratio for merged reflection intensities. [b] $R_{merge} = \sum_h\sum_l|I(h) - I_l(h)|/\sum_h\sum_l I_l(h)$, where $I_l(h)$ is the *l*th measurement and $I(h)$ is the mean measurement of reflection *h*. [c] The test set and working set of reflections are set aside for cross-validation (*36*) during refinement. [d] $R = \sum_h|F_o - F_c|/\sum_h|F_o|$, where F_o and F_c are the observed and calculated structure factor amplitudes of reflection *h*. R_{free} is *R* for the test reflection data set, R_{work} is *R* for the working reflection set, and R_{total} is *R* for all the data. [e] Root mean square difference in *B* factor for bonded atoms; m/m, m/s, and s/s represent main chain−main chain, main chain−side chain, and side chain−side chain bonds, respectively. [f] Based on the Luzzati plot (*37*) of *R* vs 2 sin θ/λ, where θ is the angle of diffraction and λ is the X-ray wavelength. [g] DPI is the diffraction data precision indicator (*38*) based on *R* or R_{free} and a rough approximation to the least-squares method.

Phase-sensitive NOESY spectra were acquired at 20 °C with mixing times ranging from 1 to 5 ms. Typical NOESY spectra were collected with 256 experiments in the F_1 dimension using the hypercomplex method of States et al. (*28*). In general, 400 scans were accumulated for each F_1 experiment, which was acquired with 4096 complex points in the F_2 dimension over a spectral width of 109.7 kHz. The residual solvent signal in all NOESY experiments was suppressed using a 20 ms presaturation with a weak decoupler power.

Clean TOCSY (*29*) spectra were recorded at 500 MHz over different spectral windows using 4096 F_2 points and 256 complex F_1 points of 320−400 scans. Solvent suppression was achieved by a 200 ms direct saturation during the relaxation delay period. Various mixing times (2, 10, 30, and 40 ms) were used to allow effective spin-lock for protons with different relaxation properties.

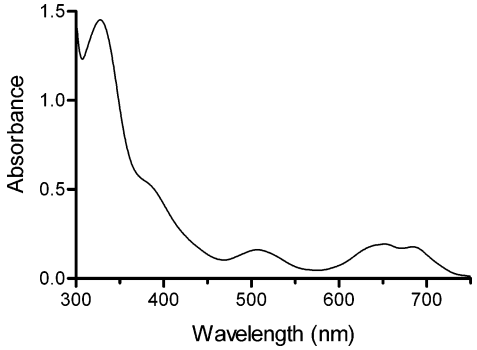

FIGURE 1: Visible absorption spectrum of cobalt(II) amicyanin. The spectrum was recorded in 0.1 M potassium phosphate buffer at pH 7.4. The concentration of cobalt(II) amicyanin was approximately 0.1 mM.

All 2D data were processed on a Dell Dimension 8200 PC with Pentium 4 processor using Felix 2002 (Accelrys, Inc.). Various apodization functions were employed to emphasize protons with different relaxation properties. For example, apodization over 256, 512, and 1024 points was used to emphasize fast-relaxing broad cross-peaks at the expense of resolution, while apodization over 2048 points is necessary to emphasize slowly relaxing cross-peaks. All 2D data were zero filled to obtain 4K × 4K 2D matrices as required by the large hyperfine shift dispersion exhibited by the paramagnetic nature of this protein.

The structures of both native and cobalt(II) amicyanin were examined on either a Silicon Graphics Indigo 2 Extreme workstation using Quanta (Accelrys, Inc.) or a Dell Dimension 8200 computer using ViewerLite (Accelrys, Inc.) to visualize crystallographic coordinates.

RESULTS

Biochemical Properties. The visible absorption spectrum of cobalt(II) amicyanin is shown in Figure 1. The features of the absorption spectrum are similar to those of other cobalt-substituted cupredoxins and, in particular, to *P. versutus* cobalt(II) amicyanin (*15*). The ligand to metal charge transfer peak is present at 328 nm, and four ligand field peaks occur with closely similar positions and relative intensities. The only difference is a pair of nearly equal ligand field peaks at 653 and 684 nm that are reversed in their relative intensities.

No spectral changes were observed after incubation of *P. denitrificans* cobalt(II) amicyanin with the reductant sodium dithionite or the oxidant hydrogen peroxide. Reduced MADH was not reoxidized by cobalt(II) amicyanin, and cobalt(II) amicyanin did not mediate electron transfer from reduced MADH to oxidized cytochrome *c*-551i. This is not surprising since cobalt(I) is not an accessible oxidation state. When cobalt(II) amicyanin was included in the steady-state assay of methylamine-dependent reduction of amicyanin by MADH inhibition was observed. The K_i value for inhibition by cobalt(II) amicyanin was 5.4 ± 0.4 μM (data not shown). This K_i value for cobalt(II) amicyanin is very similar to the K_m value for native amicyanin in the steady-state assay (*30*). This is consistent with the overall structural similarity of amicyanin and cobalt(II) amicyanin and suggests that it binds to MADH with a similar affinity. It was not previously possible to perform such an inhibition experiment with apoamicyanin since that protein is unstable in solution (*31*).

Table 2: Root Mean Square Deviations of Cα Positions

(a) RMSD of Cα Positions between the Backbones of the Four Molecules in the Asymmetric Unit of Cobalt Amicyanin[a]

chain	A (Å)	B (Å)	C (Å)
D	0.55 (0.35)	0.77 (0.27)	0.33 (0.32)
C	0.41 (0.17)	0.81 (0.44)	
B	0.56 (0.43)		

(b) RMSD of Cα Positions in the Backbones of the Four Molecules in the Asymmetric Unit of Cobalt Amicyanin Compared with the Backbone of Wild-Type Amicyanin (PDB Code 1AAC)[a]

chain	1AAC (Å)
A	0.36 (0.36)
B	0.52 (0.39)
C	0.53 (0.36)
D	0.56 (0.31)

[a] For the values in parentheses residues 17−20 are omitted from the calculation.

The observation that cobalt(II) amicyanin does not mediate electron transfer from reduced MADH to oxidized cytochrome *c*-551i indicates that the presence of a redox-active metal in amicyanin is critical for this long-range electron-transfer process.

Crystal Structure. (A) Refinement Results. The final model of cobalt(II) amicyanin consists of four independent molecules, each with 105 residues and 1 cobalt atom. Five residues display discrete disorder: Ser9 and Met71 from molecule A, Ser9 and Asp24 from molecule B, and Lys101 from molecule C. Three of the five phosphate ions are associated with molecule A. Two of these ions bind at sites that are common to the phosphate ions found in molecules B and C, respectively. The Ramachandran plot (*32*) indicates that all but one residue (Lys74 of molecule B) are in the most favored or additionally allowed regions and none are in the disallowed region of the diagram.

(B) Structure of Cobalt Amicyanin. The four independent molecules of cobalt(II) amicyanin have root mean square deviation (RMSD) values in equivalent Cα positions ranging from about 0.3 to 0.8 Å between pairs of aligned molecules (Table 2a). The largest variations among the alignments occur in the polypeptide segment 17−20 where deviations of up to 4 Å occur between Cα atoms of individual chains. When this segment is omitted from the comparison, the RMSD between molecules falls to about 0.2−0.4 Å (Table 2a). In the wild-type structure determined at 1.31 Å resolution (*4*), this segment was found to have *B* factors about twice that of the average. In cobalt(II) amicyanin, the *B* factors in these segments are approximately the same as in the rest of the respective individual molecules in the asymmetric unit, indicating that the segments are well ordered. However, the segment appears to be quite malleable and able to take up a variety of conformations as dictated by the crystal packing. These variations may reflect structural differences at the metal-binding site of amicyanin but do not appear to be directly correlated with other structural variations in the molecule. The crystal packing of cobalt amicyanin is described in the Supporting Information.

(C) Comparison of Cobalt Amicyanin with Native Amicyanin. When each of the four cobalt(II) amicyanin molecules is compared with the native protein, the RMSD of equivalent Cα positions ranges from 0.36 to 0.56 Å (Table 2b). When the polypeptide segment 17−20 is omitted from the comparison, these RMSDs range from 0.31 to 0.39 Å (Table 2b). Comparison of individual chains of the cobalt(II) amicyanin with the native protein shows consistently large deviations in Cα positions (>0.5 Å) for all four chains in segments 1, 14−15, 63−64, and 94−95. The first two regions show similar variation when comparing the four cobalt(II) amicyanin structures while the last two do not, suggesting the latter represent systematic structural differences between the two forms of the protein. Pro94 and His95 in amicyanin are surface residues located at the metal-binding site, and the conformational differences in this region undoubtedly reflect a change in the metal coordination geometry when copper(II) is replaced by cobalt(II) (see below). Gly63 and Glu64 are also surface residues but are located about 25 Å from the Pro94-His95 locus. In the native protein (*4*), Glu64 forms two hydrogen bonds with neighboring molecules in the crystal lattice that are absent in cobalt(II) amicyanin, possibly accounting for the difference.

(D) Metal Coordination. The cobalt atom coordination geometry is tetrahedral, with one face of the tetrahedron formed by coordinating atoms from His53, Cys92, and His95. The fourth ligand to cobalt is a water molecule that also forms a hydrogen bond with the main chain carbonyl group of Pro52 (Figure 2). When the structures of native and cobalt(II) amicyanin are overlaid (Figure 2), the cobalt atom is located 1.20 Å from the copper site. The S^{δ} atom from Met98 is 3.76 (±0.05) Å[3] from the cobalt atom, preventing it from being a ligand to cobalt. The average cobalt to ligand distances are as follows: Co−S^{γ} (Cys92) = 2.19 (±0.03) Å, Co−$N^{\delta 1}$ (His53) = 2.07 (±0.01) Å, Co−$N^{\delta 1}$ (His95) = 1.93 (±0.01) Å, and Co−O (H_2O) = 2.25 (±0.07) Å. The bond distances and angles of the metal coordination in copper(II) and cobalt(II) amicyanin are given in Table 3.

(E) Comparison of Cobalt Amicyanin with Cobalt Azurin. As indicated earlier, the copper coordination in native azurin from *P. aeruginosa* is a distorted trigonal bipyramid, with three equatorial side chain ligands, His46, Cys112, and His117, one axial side chain ligand, Met121, and the carbonyl oxygen of Gly45 (*9*). When the copper of azurin is replaced with cobalt, the metal coordination pattern remains essentially the same, but the metal ion moves away from the axial ligand Met121 and approaches the carbonyl ligand of Gly45 (*33*). The coordination geometry of the metal site of cobalt(II) azurin is compared to that of cobalt(II) amicyanin in Figure 3 and in Table 3. For the figure the cobalt ions and protein or water atoms to which they are coordinated in the two structures were fit by least squares. In native amicyanin, the copper coordination geometry is a distorted tetrahedron, with His53, Cys92, and His95 forming the three equatorial ligands, Met98 as the axial ligand, but no oxygen atom as a fifth ligand. On binding cobalt, the metal site moves away from the axial methionine, and a water molecule is recruited to

[3] The values for the distances between cobalt and various atoms in amicyanin are averaged over the four cobalt(II) amicyanin molecules in the asymmetric unit. The quantities within the parentheses are the mean deviations of these distances from the average.

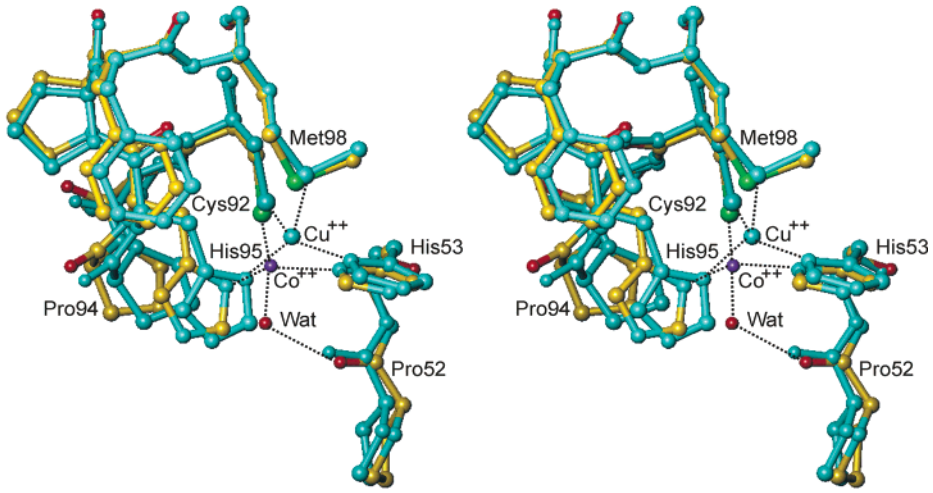

FIGURE 2: Stereoview showing a comparison of the metal-binding ligands of cobalt-substituted and native amicyanin from *P. denitrificans*. Cobalt(II) amicyanin is presented with atom colors (carbon, yellow; nitrogen, cyan; oxygen, red; sulfur, green) and copper(II) amicyanin in cyan. For both proteins residue segments Pro52−His53 and Cys92−Met98 and the metal ion (cobalt, violet; copper, cyan) are shown. The water molecule (red) that forms the fourth cobalt ligand in cobalt(II) amicyanin is also shown. This diagram was made using Turbo-Frodo (*39*).

Table 3: Metal Coordination Geometry in Native and Cobalt-Substituted Amicyanin and Azurin[a,b]

	cobalt amicyanin[c] (Å or deg)	copper amicyanin (Å or deg)	cobalt azurin (Å or deg)	copper azurin (Å or deg)
M−His53/46 N^{δ}	2.07 (0.01)	1.95	2.32	2.11
M−Cys92/112 S^{γ}	2.19 (0.03)	2.11	2.20	2.25
M−His95/117 N^{δ}	1.93 (0.01)	2.03	2.25	2.03
M−Wat/Gly O[d]	2.25 (0.07)		2.15	2.97
M−Met98/121 S^{δ}	3.76 (0.05)	2.90	3.49	3.15
∠His53/46 N^{δ}−M−Cys92/112 S^{γ}	112.1 (2.9)	136	120.1	133
∠Cys92/112 S^{γ}−M−His95/117 N^{δ}	126.8 (1.6)	112	121.7	123
∠His53/46 N^{δ}−M−His95/117 N^{δ}	113.3 (2.2)	104	117.5	103
∠His53/46 N^{δ}−M−Wat/Gly O[d]	102.6 (1.9)		79.1	73
∠Cys92/112 S^{γ}−M−Wat/Gly O[d]	100.4 (2.2)		105.2	98
∠His95/117 N^{δ}−M−Wat/Gly O[d]	95.5 (1.2)		93.4	89
∠His53/46 N^{δ}−M−Met98/121 S^{δ}	65.6 (1.0)	84	69.1	78
∠Cys92/112 S^{γ}−M−Met98/121 S^{δ}	92.4 (1.7)	110	95.8	110
∠His95/117 N^{δ}−M−Met98/121 S^{δ}	82.3 (1.6)	100	96.1	87

[a] In column 1 of the table M represents either cobalt or copper. This ligand is not present in copper amicyanin. [b] In amicyanin the metal ligands are His53, Cys92, His95, and Met98; in azurin these ligands correspond to His46, Cys112, His117, and Met121, respectively. [c] Distances and angles are the average of the four observations for cobalt amicyanin, and the values in parentheses are their observed standard deviations. [d] In cobalt azurin the oxygen ligand to the metal is the carbonyl oxygen of Gly45 rather than a water oxygen as in cobalt amicyanin.

serve as the fourth ligand. As can be seen in Figure 3 and Table 3, the equatorial ligand geometry and the axial oxygen ligand position in cobalt(II) amicyanin are nearly identical to those of cobalt(II) azurin. However, the cobalt to Met98 S^{δ} distance of 3.76 Å is about 0.25 Å longer than the comparable distance in cobalt(II) azurin, implying that no coordination bond is formed between them. Even in cobalt(II) azurin, the Met S^{δ} to cobalt distance of 3.48 Å is so long that one could question whether it contributes significantly to the metal coordination and the stability of the complex.

NMR Spectroscopy. The spectral features of cobalt(II)-substituted *P. denitrificans* amicyanin (Figure 4) display a high degree of similarity to that of the cobalt(II) derivative from *P. versutus* (*15*). The two extremely broad, fast-relaxing, strongly hyperfine-shifted signals with integrated intensities of one proton each (peaks A and B at 303 and 298 ppm) are characteristic features of protons in close proximity to the metal center. They have been tentatively assigned to the two β-protons of the metal ligand Cys92 on the basis of their extremely downfield-shifted positions, considerable large line widths, and fast longitudinal relaxation rates (Table 4). Other resonances with intensities of one proton each in the downfield region represent protons from other amino acid residues that coordinate to the metal center. The resolved upfield spectral region displays several single proton resonances and a few multiproton signals. Previous studies on several cobalt(II)-substituted cupredoxins have firmly concluded that the upfield spectral region primarily encompasses the resonances from protons of the methionine residue (*15*, *34*) despite its remote distance from the metal center (*13*).

The assignment of the hyperfine-shifted signals was achieved through comparison with the assignments made for other cobalt(II)-substituted cupredoxins and examination of the active site structure of cobalt(II) amicyanin revealed by its crystal structure, with confirmation through two-dimensional NOE measurements. Efforts to obtain contact couplings, such as traditional COSY and clean TOCSY, were unsuccessful due to the large spread of the relaxation rates and wide dispersion of the chemical shifts of the resonances.

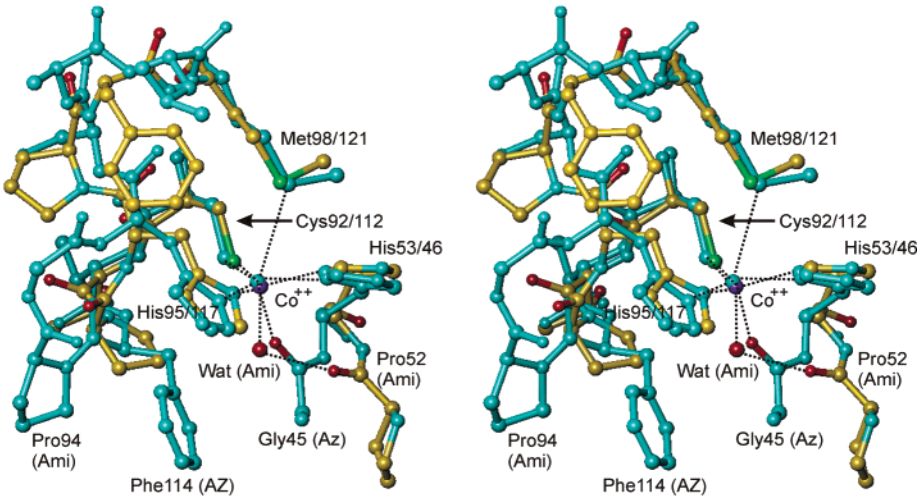

FIGURE 3: Stereoview showing a comparison of the cobalt-binding geometry of cobalt(II) amicyanin from *P. denitrificans* and cobalt(II) azurin. Cobalt(II) amicyanin is shown in atom colors (carbon, yellow; nitrogen, cyan; oxygen, red; sulfur, green) and cobalt(II) azurin in cyan, except for the carbonyl oxygen atom of Gly45, which is red. For amicyanin residue segments Pro52−His53 and Cys92−Met98 and for azurin residue segments Gly45−His46 and Cys112−Met121 are shown. For the alignment of the two structures, the cobalt ions (amicyanin, cyan; azurin, red) and the protein and water atoms in their coordination spheres were fit by least squares using Turbo-Frodo (*39*). This diagram was made using Turbo-Frodo (*39*).

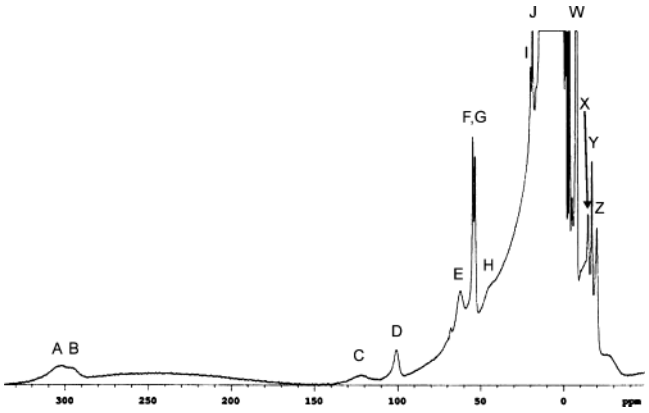

FIGURE 4: 500 MHz ^{1}H NMR spectrum of *P. denitrificans* cobalt(II) amicyanin in D_2O at 293 K in 0.1 M phosphate buffer at pH 7.4.

Table 4: Proton NMR Parameters and Assignments of Paramagnetically Shifted Resonances in *P. denitrificans* Cobalt(II) Amicyanin at 293 K in 0.1 M Phosphate Buffer, pH 7.4

	P. denitrificans		*P. versutus*[a]		
signal	δ (ppm)	T_1 (ms)	δ (ppm)	T_1 (ms)	assignment
A	303	<1	∼285	nd[b]	Cys C$^{\beta 1}$H
B	298	<1	∼285	nd[b]	Cys C$^{\beta 2}$H
C	122	<1	117.9	0.8	His C$^{\epsilon 1}$H
D	101	3.5	132.5	2.9	Met C$^{\gamma 1}$H
E	65	nd[b]			?
F	55.1	17.3	52.6	24.2	His C$^{\delta 2}$H
G	53.9	11.5	51.0	14.8	His C$^{\delta 2}$H
H	∼43	<1	37.8	∼0.8	His C$^{\epsilon 1}$H
I	20.2	11.5	21.6	16.2	?
J	18.3	23.1	18.9	24.4	Cys CαH
W	−7.4	12.7			Met C$^{\epsilon}$H$_3$
X	−14.2	2.9	−16.7	9.0	?
Y	−16.8	8.6	−16.1	8.2	Met C$^{\beta 2}$H
Z	−19.7	5.8	−18.6	4.9	Met C$^{\beta 1}$H

[a] Parameters for *P. versutus* cobalt(II) amicyanin are included for comparison. Taken from ref *15*. [b] Not determined.

The dipolar-only approach is obviously insufficient for the unambiguous assignment of signals in this paramagnetic metalloprotein. Fortunately, the characteristic spin systems of the coordinated residues in this protein and many similar studies in the literature provide clues to the signal assignments in this work. Shown in Figure 5 is the NOESY spectrum collected in D_2O buffer with a mixing time of 1.0 ms. The clear NOESY connectivities lead to the proposed assignments for most of the nonexchangeable hyperfine-shifted protons. The chemical shifts and the spin−lattice relaxation times for the hyperfine-shifted resonances and their assignments are compiled in Table 4, along with the corresponding parameters in *P. versutus* cobalt(II) amicyanin reported previously (*15*).

The fact that the two Cβ protons of the Cys ligand display clearly resolved resonances (Figure 4) suggests that the magnetic property of the metal center in *P. denitrificans* amicyanin is somewhat different from that in *P. versutus* amicyanin, that gives a single broad signal comprising the two overlapping Cβ protons of the Cys ligand (*15*). The further downfield position of the Cys proton resonances is also indicative of a stronger interaction of the Cys ligand with the metal center in the case of *P. denitrificans* amicyanin than that of the *P. versutus* protein (Table 4). The nearly identical chemical shifts of the His ligands in the two proteins implicate very similar arrangement of these ligands within the metal center in the two cobalt(II) amicyanins (Table 4).

The assignment of Met98 relies on the observation of several resonances characteristic of methionine in the upfield region of the spectrum. The distinctive spectral pattern of methionine has been firmly established for the *P. versutus* protein by the observation of NOEs between the upfield signals and the unique downfield signals of Cys (*15*). As mentioned previously, no NOEs are displayed by the Cβ protons of the Cys ligand in *P. denitrificans* amicyanin. However, the NOEs (peaks 2 and 3, Figure 5) between the upfield signals (peaks W and Y, Figure 4) and the signal at ∼100 ppm (peak D, Figure 4) suggest the assignments of these peaks to Met98 as listed in Table 4. Observation of an intense NOE between signals Y and Z (expansion of Figure 5; data not shown) confirms the assignment of these peaks to the β-protons of Met98. Assignment of one of the Met98 γ-protons is achieved by the NOE observed between peak

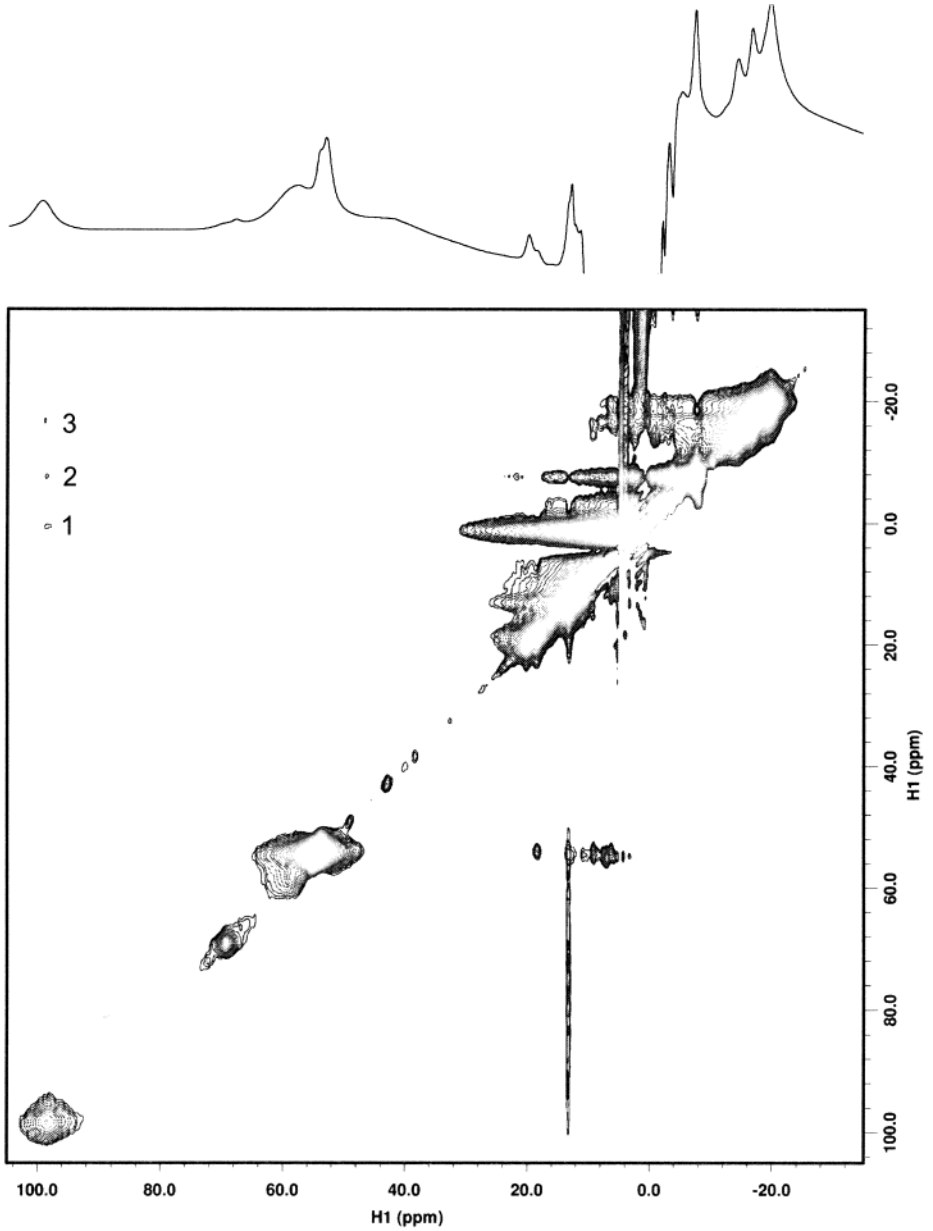

FIGURE 5: 500 MHz phase-sensitive ^{1}H NOESY spectrum of *P. denitrificans* cobalt(II) amicyanin in D_2O taken with a mixing time of 1.0 ms. Other conditions are identical to those in Figure 4. Cross-peak assignments: (1) $C^{\gamma 1}$H Met95−$C^{\gamma 2}$H Met95; (2) $C^{\gamma 1}$H Met95−$C^{\epsilon}H_3$ Met95; (3) $C^{\gamma 1}$H Met95−$C^{\beta 1}$H Met95.

D and a resonance at 0.64 ppm (cross-peak 1, Figure 5). With a distance of 3.76 Å, no coordination bond is expected between the S^{δ} atom of Met98 and the metal ion. Nonetheless, significant paramagnetic relaxation is observed on this residue. This is consistent with the observation made on cobalt(II) azurin where the Met S^{δ} to cobalt distance is too long (3.48 Å) to contribute significantly to metal coordination but short enough to experience significant paramagnetic relaxation from the metal ion (*13*).

Examination of the results in Table 4 indicates that the C^{γ} proton close to the Met98 S^{δ} ligand in *P. denitrificans* cobalt(II) amicyanin (peak D) displays a much smaller shift (∼100 ppm) than the corresponding residue in *P. versutus* cobalt(II) amicyanin (∼133 ppm). The weaker paramagnetic effects of cobalt(II) in *P. denitrificans* cobalt(II) amicyanin are indicative of a longer Co(II)−S(Met) distance than in *P. versutus* cobalt(II) amicyanin (*35*). The difference in the ligand−metal interaction in these two similar proteins could suggest a different response of the metal-binding center toward metal substitution. The crystal structure of *P. denitrificans* cobalt(II) amicyanin presented here confirms the conclusion from the NMR analysis that Met98 has moved away from the metal atom and is perhaps no longer within the coordination sphere.

DISCUSSION

Type I copper proteins have been the subject of extensive biophysical and structural studies. The bacterial protein azurin has been the primary topic of such studies. Azurin is believed to mediate electron transfer in interprotein electron transfer chains, but its specific function remains unclear. In contrast, the function of amicyanin is well established as a mediator of electron transfer from MADH to cytochromes *c*. While amicyanin is also a bacterial protein, it exhibits much greater structural similarity to the plant cupredoxin, plastocyanin, which mediates electron transfer from cytochrome *f* of the

cytochrome b_6f complex to P700 in photosystem I. The most significant structural difference in the metal-binding site of amicyanin and azurin is that in azurin the carbonyl oxygen of a glycine residue provides a fifth ligand for copper occupying a second axial position. The corresponding residue in amicyanin is a proline which is not close enough to provide such a ligand.

The crystal structure of *P. versutus* cobalt(II) amicyanin has not been reported, but this protein has been studied by paramagnetic NMR (*15*). One of the conclusions of that report was that the coordination of the cobalt ion was very similar to that of the copper ion in the native protein, i.e., 4-coordinate involving (Cys)$(His)_2$(Met) ligation. That conclusion was based on the absence of any resonances belonging to Pro52, the residue whose analogue in azurin provides a carbonyl oxygen ligand to the cobalt in cobalt azurin (*13*). The conclusion was substantiated by the presence of a strongly shifted hyperfine resonance from the $H^{\gamma 1}$ proton of Met98 that suggested a considerably stronger interaction between the methionine sulfur and the cobalt ion than was observed in cobalt azurin (*13*) and that would have resulted from the perceived absence of an oxygen ligand. Assuming that the same structural perturbations occur in *P. versutus* as in *P. denitrificans* cobalt amicyanin, the present results show that this conclusion was incorrect, since a water molecule, in fact, substitutes for the carbonyl oxygen present in azurin but could not be detected in the NMR. The present results also suggest that the strength of the cobalt/methionine interaction is weaker in the *P. denitrificans* protein than in the *P. versutus* protein, based on the smaller chemical shift attributed to the Met98 $H^{\gamma 1}$ proton (~100 vs ~130 ppm, respectively). In cobalt-substituted azurin, the chemical shift for the Met98 $H^{\gamma 1}$ proton is smaller still, ~45 ppm. This would seem to suggest that the cobalt−methionine interaction in cobalt azurin is even weaker than in *P. denitrificans* amicyanin, even though the Met S^{δ} atom is about 0.25 Å closer to cobalt in the azurin than in the amicyanin cobalt complex. It is difficult to obtain quantitative distance information from paramagnetic chemical shift data, especially in proteins of different structure. Furthermore, several factors can influence the magnitude of these shifts such as the extent of the contact and pseudocontact contributions (*13*). However, the coordination of cobalt and the orientation of the axial methionine in the two proteins are remarkably similar, as shown in Figure 3, suggesting that the chemical shifts of the methionine protons in cobalt azurin and cobalt amicyanin might be similar. The basis for the discrepancy in chemical shift between the two amicyanin NMR studies can only be known with certainty when the crystal structure of the *P. versutus* protein is known.

The results of the NMR studies of *P. denitrificans* cobalt(II) amicyanin are consistent with the crystal structure of the protein and provide verification that this structure is an accurate reflection of its structure in solution. Since metal substitution in copper and other metalloproteins is commonly used to elucidate the properties of the native protein by spectroscopic means, the present results indicate the importance of confirming the structures of such metal-substituted metalloproteins by crystallography and/or NMR. The importance of the oxygen ligand in stabilizing the binding of metals such as cobalt and nickel is highlighted by these results. In cobalt(II) azurin the glycine carbonyl oxygen ligand is strengthened as the methionine sulfur ligand weakens. In cobalt(II) amicyanin, where no such protein-derived oxygen ligand is structurally possible, water is recruited to form a new ligand when the methionine sulfur ligand weakens. Such a structural role for water has not previously been reported for a native or metal-substituted type I copper protein.

ACKNOWLEDGMENT

Use of the Advanced Photon Source was supported by the U.S. Department of Energy, Office of Science, Office of Basic Energy Sciences, under Contract W-31-109-ENG-38. We thank the staff at BIOCARS for assistance and equipment. The authors acknowledge the University of Southern Mississippi Polymer Science NMR facility for the use of the Varian Unity-Inova 500 MHz spectrometer, purchased via NSF Division of Materials Research/Major Research Instrumentation Award 0079450.

SUPPORTING INFORMATION AVAILABLE

Crystal packing analysis data, one table giving hydrogen-bonding interactions of molecules of cobalt amicyanin, and one figure showing crystal packing of cobalt amicyanin. This material is available free of charge via the Internet at http://pubs.acs.org.

REFERENCES

1. Husain, M., and Davidson, V. L. (1985) An inducible periplasmic blue copper protein from *Paracoccus denitrificans*. Purification, properties, and physiological role, *J. Biol. Chem. 260*, 14626−14629.
2. van Houwelingen, T., Canters, G. W., Stobbelaal, G., Duine, J. A., Frank, J., and Tsugita, A. (1985) Isolation and characterization of a blue copper protein from *Thiobacillus versutus*, *Eur. J. Biochem. 153*, 75−80.
3. van Spanning, R. J., Wansell, C. W., Reijnders, W. N., Oltmann, L. F., and Stouthamer, A. H. (1990) Mutagenesis of the gene encoding amicyanin of *Paracoccus denitrificans* and the resultant effect on methylamine oxidation, *FEBS Lett. 275*, 217−220.
4. Cunane, L. M., Chen, Z., Durley, R. C. E., and Mathews, F. S. (1996) X-ray crystal structure of the cupredoxin amicyanin from *Paracoccus denitrificans*, refined at 1.31 Å resolution, *Acta Crystallogr. D52*, 676−686.
5. Romero, A., Nar, H., Huber, R., Messerschmidt, A., Kalverda, A. P., Canters, G. W., Durley, R., and Mathews, F. S. (1994) Crystal structure analysis and refinement at 2.15 Å resolution of amicyanin, a type I blue copper protein, from *Thiobacillus versutus*, *J. Mol. Biol. 236*, 1196−1211.
6. Petratos, K., Banner, D. W., Beppu, T., Wilson, K. S., and Tsernoglou, D. (1987) The crystal structure of pseudoazurin from *Alcaligenes faecalis* S-6 determined at 2.9 Å resolution, *FEBS Lett. 218*, 209−214.
7. Guss, J. M., Bartunik, H., and Freeman, H. C. (1992) Accuracy and precision in protein structure analysis: Restrained least-squares refinement of the structure of poplar plastocyanin at 1.33 Å resolution, *Acta Crystallogr. B48*, 790−811.
8. Baker, E. N. (1988) Structure of azurin from *Alcaligenes denitrificans* refinement at 1.8 Å resolution and comparison of the two crystallographically independent molecules, *J. Mol. Biol. 203*, 1071−1095.
9. Nar, H., Messerschmidt, A., Huber, R., van de Kamp, M., and Canters, G. W. (1991) Crystal structure analysis of oxidized *Pseudomonas aeruginosa* azurin at pH 5.5 and pH 9.0. A pH-induced conformational transition involves a peptide bond flip, *J. Mol. Biol. 221*, 765−772.
10. La Mar, G., and de Ropp, S. (1993) NMR methodology for paramagnetic proteins, in *Biological magnetic resonance* (Berliner, L., and Reuben, J., Eds.) pp 1−78, Plenum Press, New York.

11. Kalverda, A. P., Salgado, J., Dennison, C., and Canters, G. W. (1996) Analysis of the paramagnetic copper(II) site of amicyanin by ^{1}H NMR spectroscopy, *Biochemistry 35*, 3085−3092.
12. Bertini, I., Paola, T., and Vila, A. (1993) Nuclear magnetic resonance of paramagnetic metalloproteins, *Chem. Rev. 93*, 2833−2932.
13. Donaire, A., Salgado, J., and Moratal, J. M. (1998) Determination of the magnetic axes of cobalt(II) and nickel(II) azurins from 1H NMR data: Influence of the metal and axial ligands on the origin of magnetic anisotropy in blue copper proteins, *Biochemistry 37*, 8659−8673.
14. McMillin, D. R., Rosenberg, R. C., and Gray, H. B. (1974) Preparation and spectroscopic studies of cobalt(II) derivatives of blue copper proteins, *Proc. Natl. Acad. Sci. U.S.A. 71*, 4760−4762.
15. Salgado, J., Kalverda, A. P., Diederix, R. E., Canters, G. W., Moratal, J. M., Lawler, A. T., and Dennison, C. (1999) Paramagnetic NMR investigations of Co(II) and Ni(II) amicyanin, *J. Biol. Inorg. Chem. 4*, 457−467.
16. Davidson, V. L., Jones, L. H., Graichen, M. E., Mathews, F. S., and Hosler, J. P. (1997) Factors which stabilize the methylamine dehydrogenase-amicyanin electron-transfer protein complex revealed by site-directed mutagenesis, *Biochemistry 36*, 12733−12738.
17. Davidson, V. L. (1990) Methylamine dehydrogenases from methylotrophic bacteria, *Methods Enzymol. 188*, 241−246.
18. Husain, M., and Davidson, V. L. (1986) Characterization of two inducible periplasmic c-type cytochromes from *Paracoccus denitrificans*, *J. Biol. Chem. 261*, 8577−8580.
19. Davidson, V. L., and Jones, L. H. (1991) Intermolecular electron transfer from quinoproteins and its relevance to biosensor technology, *Anal. Chim. Acta 249*, 235−240.
20. Lim, L. W., Mathews, F. S., Husain, M., and Davidson, V. L. (1986) Preliminary X-ray crystallographic study of amicyanin from *Paracoccus denitrificans*, *J. Mol. Biol. 189*, 257−258.
21. Otwinowski, Z., and Minor, W. (1997) Processing of x-ray diffraction data collected by oscillation methods, *Methods Enzymol. 276*, 307−326.
22. Winn, M. D. (2003) An overview of the CCP4 project in protein crystallography: An example of a collaborative project, *J. Synchrotron Radiat. 10*, 23−25.
23. Brünger, A. T., Adams, P. D., Clore, G. M., DeLano, W. L., Gros, P., Grosse-Kunstleve, R. W., Jiang, J. S., Kuszewski, J., Nilges, M., Pannu, N. S., Read, R. J., Rice, L. M., Simonson, T., and Warren, G. L. (1998) Crystallography & NMR system: A new software suite for macromolecular structure determination, *Acta Crystallogr. D54*, 905−921.
24. Murshudov, G., Vagin, A., and Dodson, E. (1997) Refinement of macromolecular structures by the maximum-likelyhood method, *Acta Crystallogr. D53*, 240−255.
25. McRee, D. E. (1999) XtalView/Xfit—a versatile program for manipulating atomic coordinates and electron density, *J. Struct. Biol. 125*, 156−165.
26. Inubishi, T., and Becker, E. (1983). Efficient detection of paramagnetically shifted NMR, *J. Magn. Reson. 51*, 128.
27. Pierattelli, R., Banci, L., and Turner, D. (1996) Indirect determination of magnetic susceptibility tensors in peroxidases: A novel approach to structure elucidation by NMR, *J. Biol. Inorg. Chem. 1*, 320−329.
28. States, D., Haberkorn, R., and Ruben, D. (1982) A two-dimensional nuclear overhauser experiment with pure absorption phase in four quadrants, *J. Magn. Reson. 48*, 286−292.
29. Griesinger, C., Otting, G., Wuethrich, K., and Ernst, R. (1988) Clean TOCSY for proton spin system identification in macromolecules, *J. Am. Chem. Soc. 110*, 7870−7872.
30. Brooks, H. B., Jones, L. H., and Davidson, V. L. (1993) Deuterium kinetic isotope effect and stopped-flow kinetic studies of the quinoprotein methylamine dehydrogenase, *Biochemistry 32*, 2725−2729.
31. Davidson, V. L., Graichen, M. E., and Jones, L. H. (1993) Binding constants for a physiologic electron-transfer protein complex between methylamine dehydrogenase and amicyanin. Effects of ionic strength and bound copper on binding, *Biochim. Biophys. Acta 1144*, 39−45.
32. Ramakrishnan, C., and Ramachandran, G. N. (1965) Stereochemical criteria for polypeptide and protein chain conformations. II. Allowed conformations for a pair of peptide units, *Biophys. J. 5*, 909−933.
33. Bonander, N., Vanngard, T., Tsai, L. C., Langer, V., Nar, H., and Sjolin, L. (1997) The metal site of *Pseudomonas aeruginosa* azurin, revealed by a crystal structure determination of the Co(II) derivative and Co-EPR spectroscopy, *Proteins 27*, 385−394.
34. Fernandez, C. O., Niizeki, T., Kohzuma, T., and Vila, A. J. (2003) Metal−ligand interactions in perturbed blue copper sites: A paramagnetic (1)H NMR study of Co(II)-pseudoazurin, *J. Biol. Inorg. Chem. 8*, 75−82.
35. Thanabal, V., de Ropp, S., and La Mar, G. (1987) Identification of the catalytically important amino acid residue resonances in ferric low-spin horseradish peroxidase with nuclear overhauser effect measurements, *J. Am. Chem. Soc. 109*, 7516−7525.
36. Brunger, A. T. (1992) Free R value: a novel statistical quantity for assessing the accuracy of crystal structures, *Nature 355*, 472−475.
37. Luzzati, V. (1952) Traitment statistique des erreurs dans la determination des structures cristallines, *Acta Crystallogr. 5*, 802−810.
38. Cruickshank, D. W. I. (1999) Remarks about protein structure precision, *Acta Crystallogr. D55*, 583−601.
39. Roussel, A., and Cambillau, C. (1989) Turbo-Frodo, in *Silicon graphics geometry partners directory*, pp 77−78, Silicon Graphics, Mountain View, CA.

BI049635R